



A preliminary investigation to determine the suitability of pigs as human analogues for post-mortem lipid analysis

Sharni Collins^a, Luca Maestrini^b, Maiken Ueland^a, Barbara Stuart^{a,*}

^a Centre for Forensic Science, University of Technology Sydney, 15 Broadway, Ultimo NSW 2007, Australia

^b Research School of Finance, Actuarial Studies and Statistics, The Australian National University, Kingsley St, Canberra ACT 2601, Australia

ARTICLE INFO

Keywords:

Forensic taphonomy
Chemometric analysis
Time since death
Animal models
Decomposition chemistry

ABSTRACT

The determination of time since death is a major challenge to law enforcement when faced with the discovery of human remains. This is due to the fact that decomposition is a complex, dynamic process influenced by several abiotic and biotic factors. For decades, post-mortem decomposition studies have used pigs as human analogues due to ethical and legal restrictions surrounding the use of human cadavers for such research. However, few comparative studies have been conducted to assess the suitability of these analogues. Recent forensic studies have successfully demonstrated the use of post-mortem lipids in textiles as a method to obtain vital information about decomposition process. The current investigation involved two studies: Trial 1 (summer) and Trial 2 (winter). Each trial with $n = 1$ human cadaver and $n = 2$ pigs. Samples were collected over a timeline of 105 days post-placement and analyzed using attenuated total reflectance (ATR-) Fourier-transform infrared (FTIR) spectroscopy. The data was then statistically assessed using functional principal component analysis, semi-parametric regression modeling and analysis of variance. The results demonstrated a clear statistically significant interspecies difference between pigs and humans in both trials. The preliminary implications of this study suggest that pigs are not suitable analogues for humans in decomposition research and have broader implications that caution the direct translation of decomposition data obtained from pigs to real human casework, particularly with respect to time since death estimations.

Introduction

Determination of time since death presents as a major challenge to law enforcement when faced with the discovery of human remains [1]. This is primarily due to complex relationships between biotic and abiotic factors influencing the post-mortem process [2]. Decomposition involves a series of chemical processes that result in the breakdown of soft tissues containing carbohydrates, proteins and lipids [3–6]. This process occurs immediately after death and ultimately results in the disintegration of all soft tissues, leaving dry or skeletal remains [3–6].

For decades, studies investigating post-mortem decomposition and time since death have utilized human analogues, primarily the domestic pig (*Sus domesticus*) due to ethical and legal restrictions limiting the use of human cadavers in decomposition research [3]. The use of pigs as analogues has been widely accepted in forensic science, due to anatomical similarities in the skin, digestive, and immunological systems [7–9]. As a result, the field of forensic taphonomy has become heavily saturated with information regarding the post-mortem processes

gained from pig models.

A review article published in 2020 by Matuszewski et al. [10] detailed selected cadaver studies conducted between 1955 and 2018 related to carrion ecology, forensic entomology and taphonomy. Of the studies listed, more than half were conducted on pigs and less than 10% on humans. However, with the emergence of human taphonomic research facilities, researchers have been able to directly compare the taphonomy of pigs and humans. Recent comparative studies have investigated the differences between pigs and humans with respect to adipose tissues [11], volatile organic compounds (VOCs) [12], insect succession [13–16], skeletal muscle tissue [17], soil biogeochemistry and microbiology [18] and total body scoring [19,20]. However, there remains an urgent need to continue these comparative studies in more fields, using different scientific methods in order to adequately assess whether pigs are suitable analogues for human decomposition work. Therefore, the current study aims to investigate the interspecies differences between pigs and humans using post-mortem lipids collected in textiles. Recent forensic studies [21–24] have demonstrated that textiles

* Corresponding author.

E-mail address: barbara.stuart@uts.edu.au (B. Stuart).

<https://doi.org/10.1016/j.talo.2022.100100>

Received 15 December 2021; Received in revised form 22 February 2022; Accepted 22 February 2022

Available online 24 February 2022

2666-8319/© 2022 The Authors. Published by Elsevier B.V. This is an open access article under the CC BY-NC-ND license (<http://creativecommons.org/licenses/by-nc-nd/4.0/>).

are a valuable source of physical evidence, particularly as a host for decomposition fluids rich in lipids [21–23].

Lipids contribute to approximately 60–85% of adipose tissues [4], with the predominant type being triacylglycerols [4,21,25]. The structure of triacylglycerols are comprised of three fatty acid tails attached via ester linkages to a glycerol molecule [4]. Following death, these lipids undergo hydrolysis due to enzymatic activity, resulting in the release of free fatty acids [4,21,22]. Due to their hydrophobic nature, these fatty acids are extremely persistent in the environment and are more stable when compared to other soft tissue biomarkers such as proteins, carbohydrates and nucleic acids [26]. Despite the fact that pigs and humans both contain approximately 20% adipose tissue [27], the composition and individual proportions differ greatly between species [11,28].

For the current study, cotton textile samples were examined using attenuated total reflectance (ATR) - Fourier transform infrared (FTIR) spectroscopy to measure the relative absorbance of target lipid regions. One hundred percent cotton was selected as the baseline for this work due to its known absorptive properties and feasibility for the collection of decomposition products and assessment using FTIR spectroscopy [21–23]. The ability to identify and monitor trends in the post-mortem lipids collected in textiles over the decomposition timeline and statistically assess these patterns provides a new pathway for the analysis of functional data on a time-dependant scale. This is a useful tool for forensic investigations where time since death is in question.

This preliminary study provides the first assessment of post-mortem lipids collected in textiles to examine interspecies differences between pigs and humans in the southern hemisphere.

Materials and methods

Experimental field site

This study was conducted at the Australian Facility for Taphonomic Experimental Research (AFTER), an outdoor eucalypt woodland on the Cumberland Plain in Western Sydney, New South Wales, Australia. This field site is privately owned and operated by the University of Technology Sydney (UTS). A description of the facility is documented in Knobel et al. [12]. Weather data were collected using a HOBO® U30 weather station within the AFTER site.

Donor information

Two human donors and four pig cadavers were placed in a supine position on the soil surface and allowed to decompose naturally. Trial 1 was conducted over the Australian summer – autumn period (commencing January 29, 2021) and included human donor 1 (H1), an 86-year-old male with a height of 174 cm and weight of 63 kg, giving a body mass index (BMI) [29] of 20.8. H1 was directly compared with two domestic 6-month-old pigs, one female (P1) and one male (P2), both weighing approximately 65 kg. Trial 2 was conducted over the Australian winter – spring period (commencing June 11, 2021) and included human donor 2 (H2), an 84-year-old male with a height of 182 cm and weight of 100 kg, giving a BMI of 30.2. H2 was directly compared with two domestic female 6-month-old pigs (P3 and P4) both weighing approximately 70 kg. All individuals were clothed in a 100% white cotton t-shirt as described in Collins et al. [22].

The human donors (H1 and H2) were received through the UTS Body Donation Programme, with consent provided in accordance with the New South Wales Anatomy Act (1977). Ethics approval was provided by the UTS Human Research Ethics Committee (HREC ETH15-0029). The human donors were not treated with any chemicals prior to placement at the facility and were allowed to decompose naturally.

Control sites were created for both trials, containing identically sourced clothing placed on the soil surface at AFTER at a minimum distance of 5 m from the decomposing remains, twice the minimum

recommended distance proposed by Luong et al. [30].

Photographs and visual observations were recorded for human and pigs on each sampling day. Visual decomposition was determined using the five reported stages of decomposition: fresh, bloat, active, advanced, and skeletal [5].

Sample collection

Textile samples were collected using sterilized scissors from the anterior aspect of the decomposing remains and respective control sites on a series of days from 0 to 105 days post-placement (Table S1). The scissors were thoroughly washed with acetone between each section. The textile samples were photographed, and any visible changes were documented. Each textile sample was individually packaged and labeled in a paper envelope and stored in a cooler for transportation to the laboratory. The textile samples were dried at ambient temperature to impede bacterial and fungal growth. Adhering soil and hair was also removed. The textile samples were then re-packaged into new, individually labeled envelopes and stored for a maximum of 3 months, at -18°C until further analysis.

Due to a local flooding event, the AFTER facility was closed between 19 March – 4 April 2021, which directly impacted sample collection for Trial 1 between days 42 and 70 post-placement (Table S1).

ATR-FTIR spectroscopy

ATR-FTIR spectra were obtained using a Nicolet Magna-IR 6700 spectrometer (Thermo Scientific, USA) and an ATR accessory consisting of a diamond crystal with a 45° angle of incidence. Spectra were recorded over a range of $4000\text{--}400\text{ cm}^{-1}$, with a spectral resolution of 4 cm^{-1} and averaged over 128 scans. Triplicates were taken for each textile sample and acetone was used to clean the ATR crystal between each sample. OMNIC software (version 8.2, Thermo Scientific, USA) was used to record and baseline-correct the spectra which were then exported as individual comma-separated values (CSV) files. The averaged stacked plots of the IR functions are shown in Figs. S1–S6.

The data was then further processed in accordance with the respective statistical methods (Fig. S7).

Data processing and statistical analyses

Functional principal component analysis (FPCA)

Principal component analysis (PCA) is a multivariate technique for high-dimensional data which is commonly used as a dimensionality reduction tool for exploratory data analysis and predictive models [31]. The purpose of PCA is often to compress, simplify and extract the most important information present within a dataset [32]. PCA has been applied as an exploration tool for chemometric analysis of IR data [21–23,33]. However, IR data is functional data due to the dependence of the observations over the wavenumber domain (in this case a scanning range of $4000\text{--}400\text{ cm}^{-1}$) [34]. For this reason, the use of an extension of traditional PCA, in the form of functional principal component analysis (FPCA) was selected in the current study to investigate the variation within the full functional dataset more accurately. FPCA replaces vectors with functions, covariance matrices with covariance operators, and scalar products in vector space by scalar products in square-integrable functional space [34–37].

For the FPCA, the triplicate absorbance values extracted from the CSV files were averaged to provide a single set of full spectra absorbance values as a representative for each sample collected post-placement. Two datasets were created, one for Trial 1 containing the data for H1, P1 and P2, and one for Trial 2 containing the data for H2, P3 and P4. These datasets were imported directly into the Unscrambler X (version 10.3, CAMO, Norway) statistical software to further process the data prior to FPCA. The first derivative using the Savitzky-Golay (SG) algorithm with 3 smoothing points and extended multiplicative scattering

correction (EMSC) was applied to the datasets. This processing method for ATR-FTIR spectra has previously been employed as it minimizes baseline differences [38–40]. Two FPCAs were produced in R [41] using the package *fdapace* [42], one for each trial: Trial 1 and Trial 2. The plots of eigenfunctions for each FPCA were then used to determine the bands of interest (Table S2) for further targeted statistical analysis (2.5.2 and 2.5.3). The residual plots (Figs. S8c and S9c) from the projection of the first two FPCs for each trial were used to determine that there are minimal unexplained features of the spectral profiles.

Semi-parametric regression analysis

In addition to FPCA, the functional data was also analyzed using semi-parametric regression models. The baseline corrected triplicate data obtained were used to extract maximum absorbance values within a set boundary for the IR bands of interest (Table S2) revealed from the plots of eigenfunctions of the FPCAs. Triplicate normalized absorbance ratios were then computed using an adapted method from Ueland et al. [23]. Each extracted maximum absorbance value was then normalized to the asymmetrical CH_2 stretching of the methylene chain $\sim 2920\text{ cm}^{-1}$ present in all spectra as a stable reference point as per Ueland et al. [23]. This method provided five normalised ratios: $\sim 1540\text{ cm}^{-1} / \sim 2920\text{ cm}^{-1}$, $\sim 1575\text{ cm}^{-1} / \sim 2920\text{ cm}^{-1}$, $\sim 1710\text{ cm}^{-1} / \sim 2920\text{ cm}^{-1}$, $\sim 1720\text{ cm}^{-1} / \sim 2920\text{ cm}^{-1}$ and $\sim 1745\text{ cm}^{-1} / \sim 2920\text{ cm}^{-1}$.

Semi-parametric regression models [43] in linear mixed model form were then fitted in R for the normalized ratios on a time dependant scale (days post-placement). The non-parametric components were given by O'Sullivan penalized splines [44]. The number of knots were selected using the simple default indications from Rupert et al. [45]. Regression lines and 95% confidence bands were obtained for the mean of the underlying process using Markov chain Monte Carlo (MCMC) sampling. The models were validated by checking the assumptions of normality, independence of the residuals and the appropriate convergence of MCMC chains. This analysis allowed a more targeted investigation of the post-mortem lipids on a time-dependant scale.

One-way analysis of variance

The triplicate normalized ratios computed were averaged to perform one-way analysis of variance (ANOVA) to compare the mean differences

between species groups (human v pig) within each trial. As the one-way ANOVA compares the mean differences between groups, the triplicate normalized ratios were averaged to eliminate the influence of intra-sample variation on the overall statistical significance. The ratios were log-transformed so that the assumptions of normality and homoscedasticity were not violated. Normality was tested using the Shapiro-Wilk test of the residuals and the hypothesis of equal variances was tested using the Levene test. The resulting p-values were then compared to a reference level of 0.05. Tukey honestly significant different (HSD) post-hoc tests were run to understand the source of the statistically significant differences from the one-way ANOVAs. The ANOVAs, tests for checking assumptions and post-hoc tests were performed using R in-built functions and the package 'car' [44].

Results and discussion

Environmental conditions

Mean temperature and total rainfall for the duration of the study is displayed in Fig. 1. Two trials were conducted for this study: Trial 1 (January 29, 2021 – May 14, 2021) and Trial 2 (June 11, 2021 – September 24, 2021). H1, P1 and P2 of Trial 1 experienced several rainfall events (Fig. 1) and an overall mean temperature of 19.4°C . Trial 2 experienced relatively less rainfall events and a lower overall mean temperature of 14.8°C .

Visual decomposition

The visual decomposition of the pigs and humans was considerably different between Trial 1 and Trial 2 (Fig. 2). During Trial 1, the pigs and human experienced several periods of heavy rainfall throughout the investigation and an overall mean temperature of 19.4°C (Fig. 1). When compared with P1 and P2, there was a considerable difference in the visual decomposition observed for H1 (Fig. 2). H1 progressed from the fresh stage into the bloat stage within the first 10 days post-placement, however, H1 did not experience a distinct active decay stage. Instead, H1 transitioned from bloat into an advanced decay, relatively stable state of mummification. In contrast, P1 and P2 progressed from fresh, bloat and then active decay within the first 10 days post-placement.

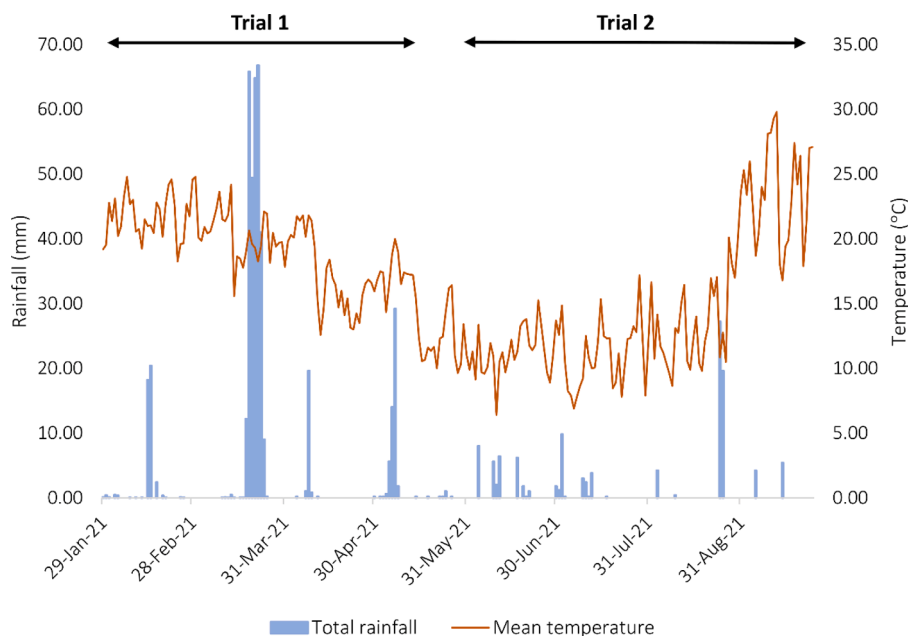


Fig. 1. Total rainfall (mm) and mean temperature ($^\circ\text{C}$) for the duration of Trial 1 and Trial 2. The overall mean temperature for Trial 1 was 19.4°C and Trial 2, 14.8°C .

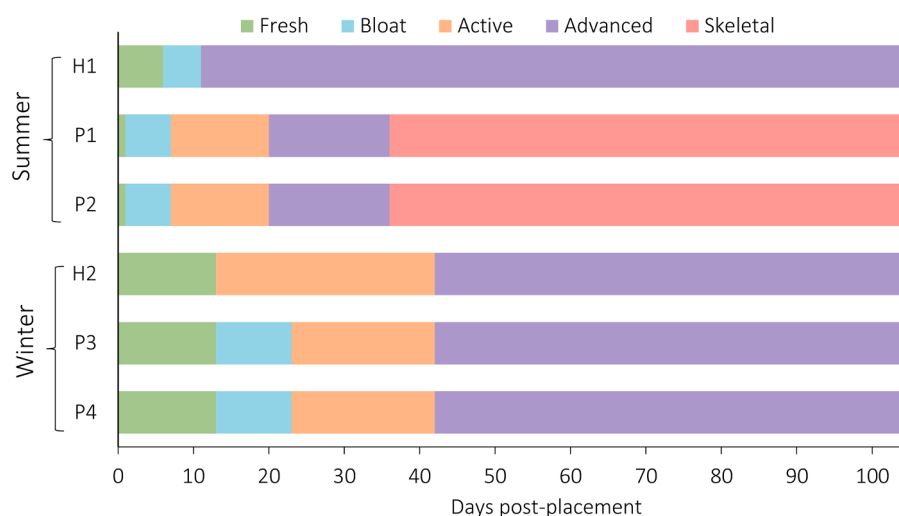


Fig. 2. Occurrence and duration of the stages of decomposition for the summer Trial 1 (H1, P1, P2) and the winter Trial 2 (H2, P3, P4) over the 105-day post-placement period.

During the active period for P1 and P2, there was dense entomological activity which is typically attributed to an abundance of volatile organic compounds (VOCs) being emitted during this stage [45]. Between days 20 and 42 post-placement, P1 and P2 reached an advanced state of decomposition with a significant loss of soft-tissue mass, resulting in skeletonization. By day 35 post-placement, both pigs were fully skeletonized (Fig. 3a and b).

Trial 2 experienced less rainfall than Trial 1 and had a lower overall mean temperature of 14.8 °C (Fig. 1). In contrast to Trial 1, there were no obvious differences in the rate and manner of which H2, P3 and P4 progressed through the stages of decomposition (Fig. 2), with the exception of H2, which did not exhibit signs of the bloat stage. By day 42 post-placement, H2, P3 and P4 had reached an advanced state of

decomposition with a large portion of soft tissue exhibiting signs of mummification (Fig. 3c and d). Overall, visual differences between the pigs and humans were evident. This occurred in both seasons, with the human not experiencing bloat in winter. However, the differences were a lot more pronounced in summer.

Textile analysis

The textile control specimens remained intact until the completion of each trial with moderate discoloration. The IR bands of interest attributed to post-mortem lipids were not visually observed in any of the control specimens throughout the duration of the trials. In contrast, the experimental samples showed considerable visual discoloration as the



Fig. 3. H1 (a) and P1 (b) from Trial 1 on day 35 post-placement. H1 in a stable state of mummification. P1 skeletonized. H2 (c) and P3 (d) from Trial 2 on day 42 post-placement. Both H2 and P3 in an advanced state of decomposition.

decomposition fluids were released from decomposing remains and absorbed into the textiles.

Functional principal component analysis (FPCA)

Trial 1

The results from the FPCA for Trial 1 (Fig. 4a) were consistent with visual observations in the field for H1, P1 and P2. The fresh sampling days for both species (0, 3 and 7 post-placement) demonstrated a clustering toward the positive portion of functional principal component 1 (FPC-1) and the negative portion of FPC-2 (Fig. 4b). The data for day 10 post-placement from H1 was projected onto the negative portion of FPC-1 and FPC-2, clearly distinguished from P1 and P2 day 10 post-placement which were projected onto the positive portion of FPC-1 and the negative portion of FPC-2. This trend was observed for the remainder of the data for Trial 1, with the data from the human (H1) being distinctly different from the pigs (P1 and P2). This provides preliminary evidence that the data obtained between humans and pigs for Trial 1 are not consistent, indicating interspecies differences.

The separation and groupings projected in the FPCA (Fig. 4a) can be explained by the eigenfunctions in the loadings plot (Fig. 4c). It is clear that the carbonyl region pertaining to the 1710, 1720 and 1745 cm^{-1} bands were responsible for the vertical spread of the data along FPC-2 (Fig. 4c). In contrast, it appeared that the C—H stretching band 2920 cm^{-1} was responsible for majority of the dispersion in the data along FPC-1 (Fig. 4c). During the decomposition process, the post-mortem lipids breakdown from larger triacylglycerols ($\sim 1745 \text{ cm}^{-1}$) and release smaller free fatty acids ($\sim 1710 \text{ cm}^{-1}$) into the immediate environment, explaining this dispersion. The data shown in Fig. 4a between day 10 and 42 post-placement corresponds to this pattern of lipid breakdown and provides evidence that this information is being effectively captured in the associated textile samples collected in-field (Fig. 4c).

The data obtained from the final two sampling days (70 and 105

post-placement) from both pig and human were more closely related to the initial cluster (Fig. 4b) than the rest of the data. This is likely due to a lower relative amount of post-mortem lipids present in the textile samples collected on those days. The loadings plot (Fig. 4c) demonstrated that this trend is due to the data from days 70 and 105 post-placement for H1, P1 and P2 containing lower relative amounts of the $\sim 2920 \text{ cm}^{-1}$ band corresponding to CH_2 asymmetrical stretching of the methylene chain, similar to the data obtained from the earlier days (Fig. 4b). In addition, the loadings plot (Fig. 4c) revealed that the data obtained from P1 and P2 for days 70 and 105 post-placement contained higher relative amounts of the ~ 1540 and $\sim 1575 \text{ cm}^{-1}$ bands corresponding to the C—O stretching from carboxylate bands of fatty acid salts. The $\sim 1710 \text{ cm}^{-1}$ band relates to the C=O stretch of free fatty acids and the lower relative amounts of the $\sim 1745 \text{ cm}^{-1}$ band is consistent with the decreased C=O stretch of triacylglycerols.

The data obtained from day 105 post-placement for H1 was grouping with the data obtained from day 10 post-placement from both P1 and P2 in the positive portion of FPC-1 and the negative portion of FPC-2. This correlates to the visual trends observed in-field, as the pigs decomposed at a much more accelerated rate than the human. This grouping provides further preliminary evidence to support the fact that there are considerable interspecies differences, particularly in respect to the decomposition timeline.

Trial 2

The FPCA for Trial 2 (Fig. 5a) is also congruent with the visual observations that were made in-field for H2, P3 and P4 with respect to the stages of decomposition. When compared to Trial 1, the data for both human and pigs were more closely related for the early decomposition period (Fig. 5b). Due to the lower temperatures observed (compared to Trial 1), there was a delay in the initial onset of visual decomposition from fresh into bloat, or active for both species. This was apparent with the large clustering toward the positive portion of FPC-1 and the negative portion of FPC-2 (Fig. 5b) that captured data from day 0 up until

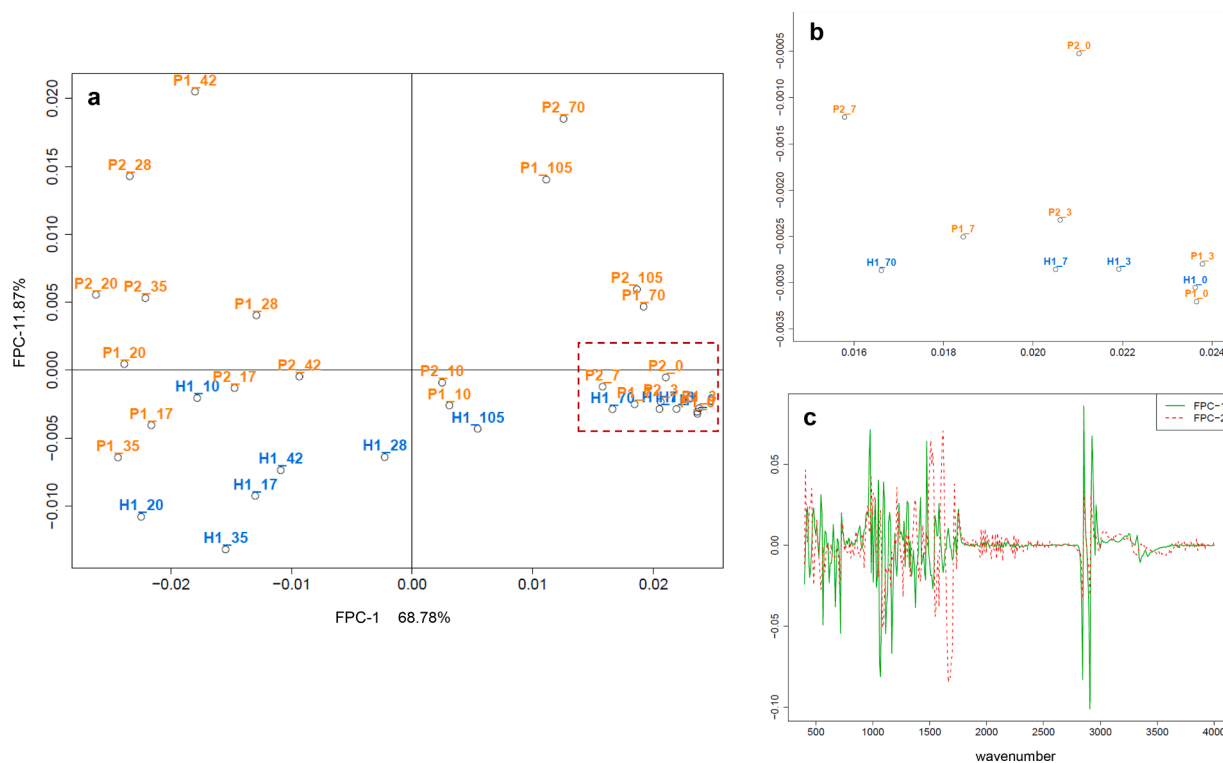


Fig. 4. Functional principal component analysis of the data observed for H1, P1 and P2 of Trial 1. Each data point represents the averaged triplicate function for each day post-placement. The red dashed box in (a) represents expanded portion displayed in (b). Plot of the eigenfunctions (c) of the processed correlation matrix for Trial 2 for FPC-1 and FPC-2 that capture 80.65% of the variation. The x-axis represents the wavenumber (cm^{-1}).

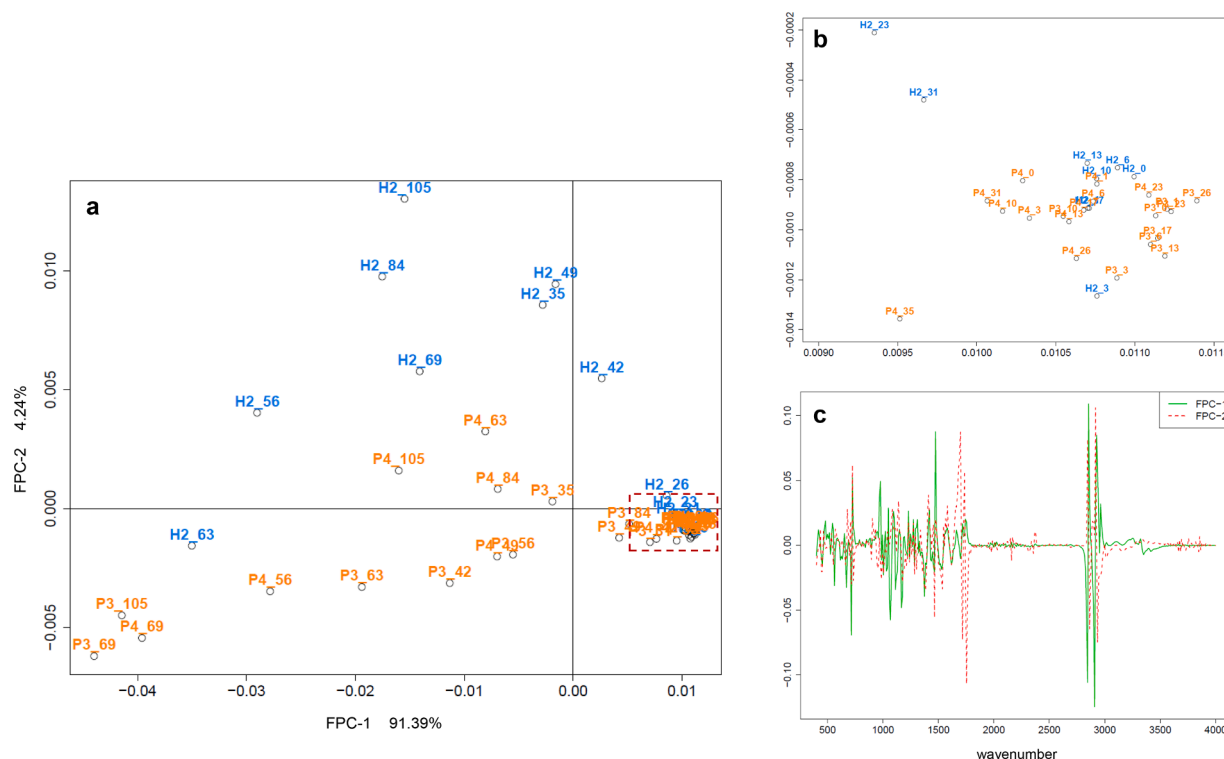


Fig. 5. Functional principal component analysis of the data observed for H2, P3 and P4 of Trial 2. Each data point represents the averaged triplicate function for each day post-placement. The red dashed box in (a) represents expanded portion displayed in (b). Plot of the eigenfunctions (c) of the processed correlation matrix for Trial 1 for FPC-1 and FPC-2 that capture 95.63% of the variation. The x-axis represents the wavenumber (cm^{-1}).

approximately day 31 post-placement for both species. This is considerably different to what was seen in Trial 1 (Fig. 4b) for H1, P1 and P2, as the early grouping only contained data from days 0 to 3 post-placement. Again, this is likely attributed to the warmer temperatures during the summer Trial 1.

In contrast to Trial 1, the data from the last sampling day (105 post-placement) was clearly distinguishable from the early cluster, with obvious differences in the data obtained from H2 projected in the negative portion of FPC-1 and the positive portion of FPC-2, and P3 projected in the negative portion of both FPC-1 and FPC-2. Overall, the patterns in the FPCAs demonstrate clear interspecies differences, particularly for the data obtained during the later decomposition period.

Several studies have demonstrated the benefit of chemometric analysis via ordinary PCA for IR data [22,23,33]. However, as previously mentioned, the application of ordinary PCA for functional data has its limitations [31,34]. The results of the current study demonstrate the successful application and interpretation of FPCAs for functional IR data. Overall, the plots of eigenfunctions from the FPCAs of Trial 1 and Trial 2 (Figs. 4c and 5c) revealed six IR bands of interest for further statistical investigation: ~ 1540 , ~ 1575 , ~ 1710 , ~ 1720 , ~ 1745 and ~ 2920 cm^{-1} .

Semi-parametric regression modeling

In order to further investigate the post-mortem lipid interspecies differences, semi-parametric regression models were fitted. These models were applied to five different band ratios: ~ 1540 cm^{-1} / ~ 2920 cm^{-1} , ~ 1575 cm^{-1} / ~ 2920 cm^{-1} , ~ 1710 cm^{-1} / ~ 2920 cm^{-1} , ~ 1720 cm^{-1} / ~ 2920 cm^{-1} and ~ 1745 cm^{-1} / ~ 2920 cm^{-1} on a time-dependant scale (day post-placement). The ~ 2920 cm^{-1} C-H stretching band was selected as the normalization factor as per Ueland et al. [23] and supported by Stuart et al. [46]. For each ratio and donor or pig, the model parameter estimates were used to produce a continuous ratio mean estimate over time and its 95% confidence bands. The residual

scatter plots from the semi-parametric regressions (Figs. S10 and S11) show that the residuals are overall randomly distributed, which confirms that the selected model fits the data in most cases. However, in some cases, such as (Fig. S10 h), extreme values, as seen on day 35 post-placement for the ratio $\sim 1710/2920$ cm^{-1} are not well captured by the models.

Trial 1

The mean daily ratios of the post-mortem lipid bands for H1 (Fig. 6a, d,g,j,m) all exhibited a spike in relative absorbance within the first 20 days post-placement, except for ~ 1710 $\text{cm}^{-1}/\sim 2920$ cm^{-1} , which peaked at approximately day 40 post-placement. In contrast, the models for P1 (Fig. 6b,e,h,k,n) and P2 (Fig. 6c,f,i,l,o) did not exhibit this spike during the early period and were generally more stable over the decomposition timeline than H1. This was most pronounced when comparing the free fatty acid ratio ~ 1710 $\text{cm}^{-1}/\sim 2920$ cm^{-1} between species (Fig. 6g–i). The ratios corresponding to the carboxylate bands of the fatty acid salts ~ 1540 $\text{cm}^{-1}/\sim 2920$ cm^{-1} and ~ 1575 $\text{cm}^{-1}/\sim 2920$ cm^{-1} demonstrated the most contrasting results between species. The mean of the underlying process of the relative absorbance for H1 for the carboxylate bands did not exceed 0.6 (Fig. 6a and d), whereas the mean of the underlying process of the relative absorbance for P1 (Fig. 6b and e) and P2 (Fig. 6c and f) far exceeded 0.6 by the final sampling day (105 post-placement). The presence of the ~ 1540 $\text{cm}^{-1}/\sim 2920$ cm^{-1} and ~ 1575 $\text{cm}^{-1}/\sim 2920$ cm^{-1} bands are indicative of adipocere formation, which is known to be a late-stage decomposition product [21,46,47]. This product is a waxy substance formed by the hydrolysis and hydrogenation of adipose tissues [46,47]. The results of the semi-parametric regression models provided evidence to support the formation of adipocere during the early stages of decomposition for P1 (Fig. 6b and e) and P2 (Fig. 6c and f) which continued to increase over the decomposition timeline. In contrast to the semi-parametric regression models for H1 (Fig. 6a and d) which provided poor evidence of this same finding.

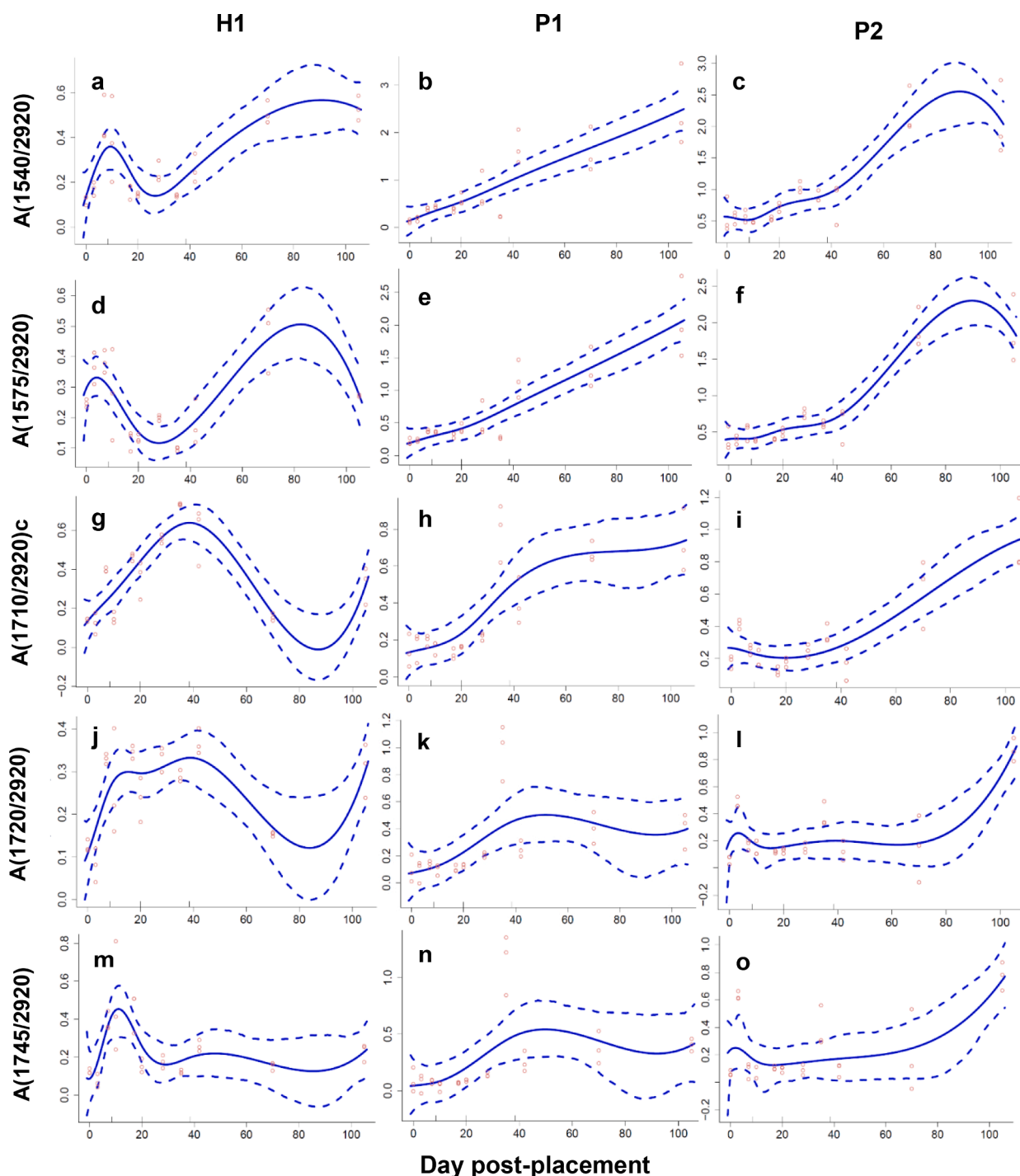


Fig. 6. Semi-parametric regression models for Trial 1 of the five normalised post-mortem lipid ratios: $\sim 1540\text{ cm}^{-1}/\sim 2920\text{ cm}^{-1}$, $\sim 1575\text{ cm}^{-1}/\sim 2920\text{ cm}^{-1}$, $\sim 1710\text{ cm}^{-1}/\sim 2920\text{ cm}^{-1}$, $\sim 1720\text{ cm}^{-1}/\sim 2920\text{ cm}^{-1}$ and $\sim 1745\text{ cm}^{-1}/\sim 2920\text{ cm}^{-1}$. The y-axis represents the normalised absorbance values, and the x-axis represents the sample period (days post-placement). The red circles represent the normalised absorbance values per sampling day. The solid blue line represents the daily mean of the underlying process, and the dashed blue lines represent the 95% confidence bands.

Trial 2

In contrast to Trial 1, the mean of the underlying process for the carboxylate bands of fatty acid salts $\sim 1540\text{ cm}^{-1}/\sim 2920\text{ cm}^{-1}$ and $\sim 1575\text{ cm}^{-1}/\sim 2920\text{ cm}^{-1}$ showed a general decreasing trend for Trial 2 (Fig. 7a–f), particularly for H2 (Fig. 7a and d). The models for the formation of free fatty acids $\sim 1710\text{ cm}^{-1}/\sim 2920\text{ cm}^{-1}$ over the decomposition timeline for H2 (Fig. 7g) and P4 (Fig. 7i) were more similar to each other than P3 (Fig. 7h), with a clear increasing trend over the decomposition timeline. The semi-parametric regression model of

the free fatty acid band, $\sim 1710\text{ cm}^{-1}/\sim 2920\text{ cm}^{-1}$, for P3 (Fig. 7h) spiked within the first few days, providing evidence of post-mortem lipid degradation from triacylglycerols to free fatty acids during the early period. Additionally, there was an increase in the release of triacylglycerols, $\sim 1745\text{ cm}^{-1}/\sim 2920\text{ cm}^{-1}$, into the textiles for H2 (Fig. 7m) around day 40 post-placement which was not observed for P3 or P4. This is likely due to differences in the rate and manner of decomposition between species.

The results of the semi-parametric regression models of the

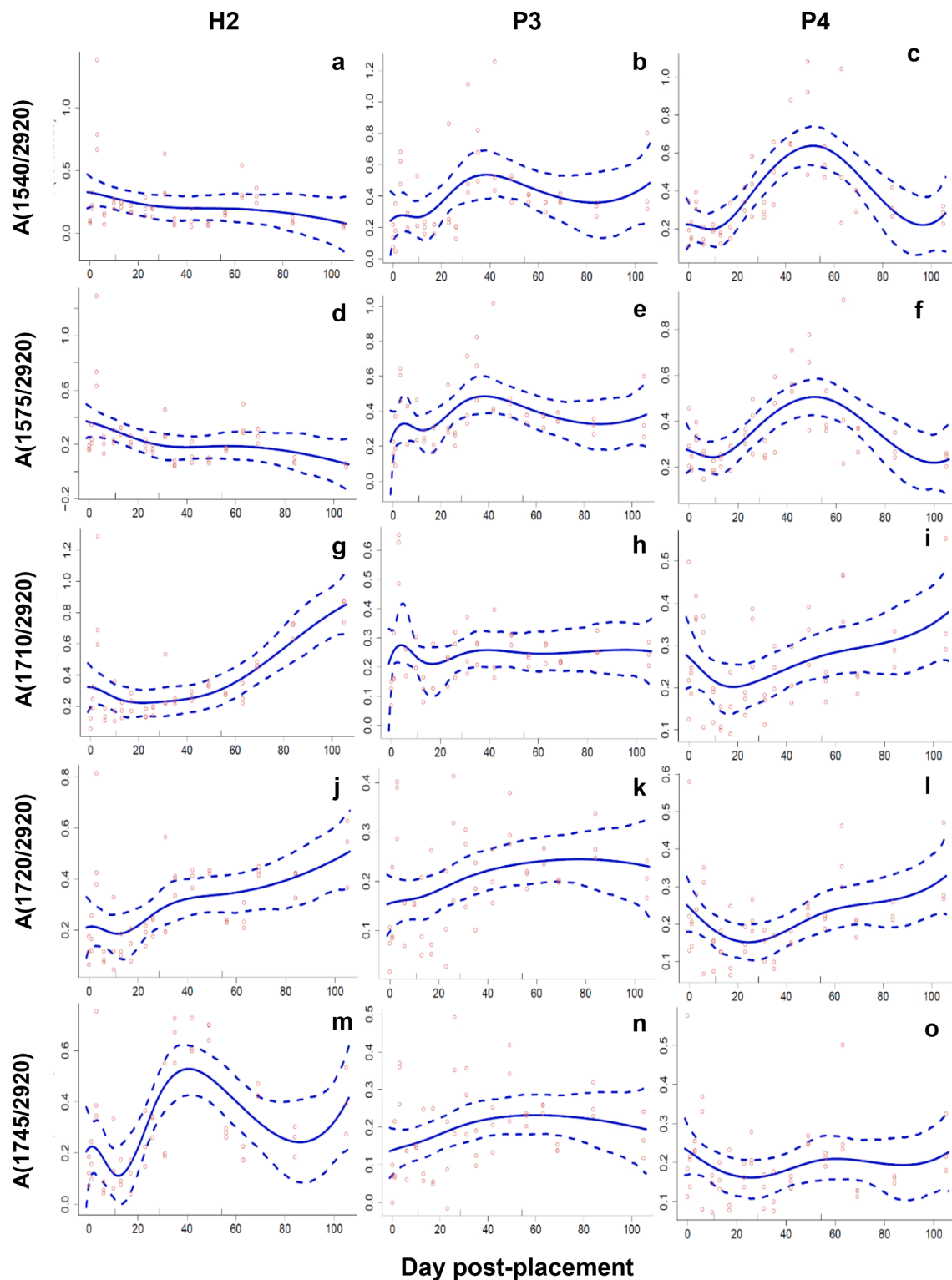


Fig. 7. Semi-parametric regression models for Trial 2 of the five normalised post-mortem lipid ratios: $\sim 1540\text{ cm}^{-1}/\sim 2920\text{ cm}^{-1}$, $\sim 1575\text{ cm}^{-1}/\sim 2920\text{ cm}^{-1}$, $\sim 1710\text{ cm}^{-1}/\sim 2920\text{ cm}^{-1}$, $\sim 1720\text{ cm}^{-1}/\sim 2920\text{ cm}^{-1}$ and $\sim 1745\text{ cm}^{-1}/\sim 2920\text{ cm}^{-1}$. The y-axis represents the normalised absorbance values, and the x-axis represents the sample period (days post-placement). The red circles represent the normalised absorbance values per sampling day. The solid blue line represents the daily mean of the underlying process, and the dashed blue lines represent the 95% confidence bands.

normalised post-mortem lipid bands for Trial 1 and Trial 2 clearly indicate interspecies differences over the decomposition period, particularly for the carboxylate bands of fatty acid salts attributed to the formation of adipocere.

Analysis of variance (ANOVA)

One-way ANOVA was performed on the daily averaged normalized ratios (Table S3) used in the semi-parametric regression modeling to statistically assess the mean differences between species groups (human

or pig) within each trial. Statistically significant results were obtained between the two species for Trial 1 and Trial 2 for the ratios corresponding to carboxylate bands of the fatty acids $\sim 1540/2920$ and $\sim 1575/2920$ (Table S3). Post-hoc tests revealed that the statistically significant differences for Trial 1 were between H1 and P1, H1 and P2 and not between P1 and P2 (Table S3). Similarly, the post-hoc tests for Trial 2 showed statistically significant differences between H2 and P3, H2 and P4 and not between P3 and P4. The results of these tests provide strong evidence to support the fact that pigs and humans decompose incongruously as the post-mortem lipids collected in textiles demonstrate clear significant differences.

Conclusions

The current study has demonstrated the successful application of FPCA to IR data as a dimensionality reduction tool, to reveal underlying patterns in the data collected from cotton textiles associated with decomposing human and pig remains. The FPCA results indicated that post-mortem lipids collected in cotton textiles were the primary influence on the variability within the datasets. In addition, the separation and groupings projected in the FPCAs could be directly correlated to both the visual in-field observations and environmental data recorded.

The application of regression modeling was also explored in this study through the use of semi-parametric regression models of normalized post-mortem lipid bands to obtain the mean of the underlying process using Markov chain Monte Carlo (MCMC). The results from these models clearly indicate interspecies differences between pigs and humans over the decomposition period, particularly for the carboxylate bands of fatty acid salts attributed to the presence of adipocere. The results from these models also provided sufficient evidence to support the use of normalized lipid ratios to monitor the chemical decomposition on a time-dependant scale. With further studies and an expansion of the current database, these models provide the potential application for casework where unknown textile evidence is yielded. In a forensic context, this could prove to be a useful tool for determining a relative post-mortem interval period, a vital aspect of complex death investigations [1].

Further statistical analysis of the averaged normalized post-mortem lipids bands was conducted via one-way ANOVA. These tests revealed statistically significant interspecies differences for the summer Trial 1 and the winter Trial 2 for the normalized ratios corresponding to the C=O stretch of the carboxylate bands of fatty acid salts at $\sim 1540\text{ cm}^{-1}/\sim 2920\text{ cm}^{-1}$ and $\sim 1575\text{ cm}^{-1}/\sim 2920\text{ cm}^{-1}$. No other normalized ratios for Trial 1 or Trial 2 revealed statistically significant results. These findings provide strong evidence to question the suitability of pigs as human analogues for taphonomic investigation as the lipid contents of the adipose tissues are not consistent between species over the decomposition period.

Overall, the results of this study provide preliminary evidence that pigs are not statistically interchangeable analogues for human decomposition with respect to post-mortem lipids collected in textiles in an Australian summer or winter season. It is important to recognize that there were several uncontrollable and systematic differences between the pigs and humans used in each trial including age, sex, cause of death and mass which could have influenced the findings. Such factors are difficult to control when conducting decomposition studies including human donors. Recommendations for future investigations include further comparative studies to adequately assess the influence of these systematic differences with an increased sample size.

In addition, the assessment of different textile types to determine the universality of this method. In particular, synthetic varieties such as polyester, which contains a sharp ester band in the carbonyl region of the infrared spectrum, would likely impact the investigation of the free fatty acids and triacylglycerols at ~ 1710 and $\sim 1745\text{ cm}^{-1}$ [22,33].

Funding

This research was funded by the Australian Research Council, the Australian Government Research Training Program and the University of Technology Sydney.

CRediT authorship contribution statement

Sharni Collins: Conceptualization, Methodology, Validation, Formal analysis, Investigation, Writing – original draft, Writing – review & editing. **Luca Maestrini:** Methodology, Software, Formal analysis, Writing – review & editing. **Maiken Ueland:** Conceptualization, Methodology, Writing – review & editing, Supervision. **Barbara Stuart:** Conceptualization, Methodology, Writing – review & editing, Supervision.

Declaration of Competing Interest

The authors declare that they have no known competing financial interests or personal relationships that could have appeared to influence the work reported in this paper.

Acknowledgments

The authors are indebted to the donors involved in the research at AFTER and their families. Without this valuable contribution, this work would not be possible. The authors would also like to thank the technical and surgical staff at UTS involved in the AFTER program.

Supplementary materials

Supplementary material associated with this article can be found, in the online version, at [doi:10.1016/j.talo.2022.100100](https://doi.org/10.1016/j.talo.2022.100100).

References

- [1] S.L. Forbes, Time since death: a novel approach to dating skeletal remains, *Aust. J. Forensic Sci.* 36 (2004) 67–72, <https://doi.org/10.1080/00450610409410599>.
- [2] E.R. Hyde, D.P. Haarmann, A.M. Lynne, S.R. Bucheli, J.F. Petrosino, The living dead: bacterial community structure of a cadaver at the onset and end of the bloat stage of decomposition, *PLoS One* 8 (2013), <https://doi.org/10.1371/journal.pone.0077733>.
- [3] M.A. Iqbal, M. Ueland, S.L. Forbes, Recent advances in the estimation of post-mortem interval in forensic taphonomy, *Aust. J. Forensic Sci.* 52 (2020) 107–123, <https://doi.org/10.1080/00450618.2018.1459840>.
- [4] B.H. Stuart, Decomposition chemistry: overview, analysis, and interpretation, in: J. A. Siegel, P.J. Saukko, M.M. Houck (Eds.), *Encyclopedia of Forensic Sciences*, 2nd ed., Academic Press, 2013, pp. 11–15.
- [5] J.A. Payne, A summer carrion study of the abpy pig *sus scrofa linnaeus*, *Ecology* 46 (1965) 592–602, <https://doi.org/10.2307/1934999>.
- [6] A.A. Vass, S.A. Barshick, G. Segal, J. Carlton, J. Love, J. Synsteli, Decomposition chemistry of human remains: a new methodology for determining the postmortem interval, *J. Forensic Sci.* 47 (2002) 542–553, <https://doi.org/10.1520/JFS15294J>.
- [7] H.J. Rothkott, Anatomical particularities of the porcine immune system—a physician's view, *Dev. Comp. Immunol.* 33 (2009) 267–272, <https://doi.org/10.1016/j.dci.2008.06.016>.
- [8] F. Meurens, A. Summerfield, H. Nauwynch, L. Saif, V. Gerds, The pig: a model for human infectious diseases, *Trends Microbiol.* 20 (2012) 50–57, <https://doi.org/10.1016/j.tim.2011.11.002>.
- [9] K.H. Mair, C. Sedlak, T. Käser, A. Pasternak, B. Levast, W. Gerner, A. Saalmüller, A. Summerfield, V. Gerds, H.L. Wilson, F. Meurens, The porcine innate immune system: an update, *Dev. Comp. Immunol.* 45 (2014) 321–343, <https://doi.org/10.1016/j.dci.2014.03.022>.
- [10] S. Matuszewski, M.J.R. Hall, G. Moreau, K.G. Schoenly, A.M. Tarone, M.H. Villet, Pigs vs people: the use of pigs as analogues for humans in forensic entomology and taphonomy research, *Int. J. Legal Med.* 134 (2020) 793–810, <https://doi.org/10.1007/s00414-019-02074-5>.
- [11] S.J. Notter, B.H. Stuart, R. Rowe, N. Langlois, The initial changes of fat deposits during the decomposition of human and pig remains, *J. Forensic Sci.* 54 (2009) 195–201, <https://doi.org/10.1111/j.1556-4029.2008.00911.x>.
- [12] Z. Knobel, M. Ueland, K.D. Nizio, D. Patel, S.L. Forbes, A comparison of human and pig decomposition rates and odour profiles in an Australian environment, *Aust. J. Forensic Sci.* 51 (2019) 557–572, <https://doi.org/10.1080/00450618.2018.1439100>.

- [13] B.M. Dawson, P.S. Barton, J.F. Wallman, Contrasting insect activity and decomposition of pigs and humans in an Australian environment: a preliminary study, *Forensic Sci. Int.* 316 (2020), 110515, <https://doi.org/10.1016/j.forsciint.2020.110515>.
- [14] Y. Wang, M.Y. Ma, X.Y. Jiang, J.F. Wang, L.L. Li, X.J. Yin, M. Wang, Y. Lai, L. Y. Tao, Insect succession on remains of human and animals in Shenzhen, China, *Forensic Sci. Int.* 271 (2017) 75–86, <https://doi.org/10.1016/j.forsciint.2016.12.032>.
- [15] K. Schoenly, N. Haskell, D. Mills, C. Bieme-Ndi, K. Larsen, Y. Lee, Recreating death's acre in the school yard: using pig carcasses as model corpses, to teach concepts of forensic entomology & ecological succession, *Am. Biol. Teach.* 68 (2006) 402–410, <https://doi.org/10.2307/4452028>.
- [16] A. Whitaker, Development of Blowflies (Diptera: Calliphoridae) on Pig and Human Cadavers: Implications For Forensic Entomology Casework, King's College London (University of London), 2014. Doctoral dissertation.
- [17] K.L. Stokes, S.L. Forbes, M. Tibbett, Human versus animal: contrasting decomposition dynamics of mammalian analogues in experimental taphonomy, *J. Forensic Sci.* 58 (2013) 583–591, <https://doi.org/10.1111/1556-4029.12115>.
- [18] J.M. DeBruyn, K.M. Hoeland, L.S. Taylor, J.D. Stevens, M.A. Moats, S. Bandopadhyay, S.P. Dearth, H.F. Castro, K.K. Hewitt, S.R. Campagna, A. M. Dautartas, G.M. Vidoli, A.Z. Mundorff, D.W. Steadman, Comparative decomposition of humans and pigs: soil biogeochemistry, microbial activity and metabolomic profiles, *Front. Microbiol.* 11 (2021), 608856, <https://doi.org/10.3389/fmicb.2020.608856>.
- [19] M. Connor, C. Baigent, E.S. Hansen, Testing the use of pigs as human proxies in decomposition studies, *J. Forensic Sci.* 63 (2018) 1350–1355, <https://doi.org/10.1111/1556-4029.13727>.
- [20] A. Dautartas, M.W. Kenyhercz, G.M. Vidoli, L.M. Jantz, A. Mundorff, D. W. Steadman, Differential decomposition among pig, rabbit, and human remains, *J. Forensic Sci.* 63 (2018) 1673–1683, <https://doi.org/10.1111/1556-4029.13784>.
- [21] S. Collins, B.H. Stuart, M. Ueland, Monitoring human decomposition products collected in clothing: an infrared spectroscopy study, *Aust. J. Forensic Sci.* 52 (2020) 428–438, <https://doi.org/10.1080/00450618.2019.1593504>.
- [22] S. Collins, B.H. Stuart, M. Ueland, Anatomical location dependence of human decomposition products in clothing, *Aust. J. Forensic Sci.* (2021) 1–13, <https://doi.org/10.1080/00450618.2021.1981443>.
- [23] M. Ueland, K.D. Nizio, S.L. Forbes, B.H. Stuart, The interactive effect of the degradation of cotton clothing and decomposition fluid production associated with decaying remains, *Forensic Sci. Int.* 255 (2015) 56–63, <https://doi.org/10.1016/j.forsciint.2015.05.029>.
- [24] F. Zapata, M.A.F. de la Ossa, C. García-Ruiz, Differentiation of body fluid stains on fabrics using external reflection Fourier transform infrared spectroscopy (FT-IR) and chemometrics, *Appl. Spectrosc.* 70 (2016) 654–665, <https://doi.org/10.1177/0003702816631303>.
- [25] M. Ueland, S. Collins, L. Maestrini, S.L. Forbes, S. Luong, Fresh vs. frozen human decomposition—a preliminary investigation of lipid degradation products as biomarkers of post-mortem interval, *Forensic Chem.* 24 (2021), 100335, <https://doi.org/10.1016/j.forc.2021.100335>.
- [26] G. Eglinton, G.A. Logan, R.P. Ambler, J.J. Boon, W.R.K. Perizonius, Molecular preservation [and discussion], *Philos. Trans. R. Soc. Lond. B Biol. Sci.* 333 (1991) 315–328, <https://www.jstor.org/stable/55419>.
- [27] S. Meeuwse, G.W. Horgan, M. Elia, The relationship between BMI and percent body fat, measured by bioelectrical impedance, in a large adult sample is curvilinear and influenced by age and sex, *Clin. Nutr.* 29 (2010) 560–566, <https://doi.org/10.1016/j.clnu.2009.12.011>.
- [28] K.L. Miles, D.A. Finaughty, V.E. Gibbon, A review of experimental design in forensic taphonomy: moving towards forensic realism, *Forensic Sci. Res.* 5 (2020) 249–259, <https://doi.org/10.1080/20961790.2020.1792631>.
- [29] A. Misra, N.V. Dhurandhar, Current formula for calculating body mass index is applicable to Asian populations, *Nutr. Diabetes* 9 (2019) 3, <https://doi.org/10.1038/s41387-018-0070-9>.
- [30] S. Luong, S.L. Forbes, J.F. Wallman, R.G. Roberts, Monitoring the extent of vertical and lateral movement of human decomposition products through sediment using cholesterol as a biomarker, *Forensic Sci. Int.* 285 (2018) 93–104, <https://doi.org/10.1016/j.forsciint.2018.01.026>.
- [31] R. Viviani, G. Grön, M. Spitzer, Functional principal component analysis of fMRI data: functional PCA of fMRI Data, *Hum. Brain Mapp.* 24 (2005) 109–129, <https://doi.org/10.1002/hbm.20074>.
- [32] H. Abdi, L.J. Williams, Principal component analysis, *Wiley Interdiscip. Rev. Comput. Stat.* 2 (2010) 433–459, <https://doi.org/10.1002/wics.101>.
- [33] M. Ueland, J.M. Howes, S.L. Forbes, B.H. Stuart, Degradation patterns of natural and synthetic textiles on a soil surface during summer and winter seasons studied using ATR-FTIR spectroscopy, *Spectrochim. Acta A Mol. Biomol.* 185 (2017) 69–76, <https://doi.org/10.1016/j.saa.2017.05.044>.
- [34] C. Hernández-Murillo, S. García, P. Fernández, M. Ménager, M.L. Montero, Integrated mineralogical and typological study of axe-god pendants from the Jade and pre-Columbian culture museum in Costa Rica, *Cuad. Antropol.* 31 (2021) 1–17, <https://doi.org/10.15517/cat.v31i1.47146>.
- [35] H.L. Shang, A survey of functional principal component analysis, *ASTA Adv. Stat. Anal.* 98 (2014) 121–142, <https://doi.org/ezproxy.lib.uts.edu.au/10.1007/s10182-013-0213-1>.
- [36] R. Burfield, C. Neumann, C.P. Saunders, Review and application of functional data analysis to chemical data—the example of the comparison, classification, and database search of forensic ink chromatograms, *Chemom. Intell. Lab. Syst.* 149 (2015) 91–106, <https://doi.org/10.1016/j.chemolab.2015.07.006>.
- [37] M. Febrero-Bande, M.O. de la Fuente, Statistical computing in functional data analysis: the R package fda.usc, *J. Stat. Softw.* 51 (2012) 1–28, <https://doi.org/10.18637/jss.v051.i04>.
- [38] M.S. Faelelbom Khairi, A. Saleh, R. Mansour, S. Sadik, First derivative ATR-FTIR spectroscopic method as a green tool for the quantitative determination of diclofenac sodium tablets, *F1000Res* 9 (2020), <https://doi.org/10.12688/f1000research.22274.2>.
- [39] B. Zimmermann, A. Kohler, Optimizing savitzky-golay parameters for improving spectral resolution and quantification in infrared spectroscopy, *Appl. Spectrosc.* 67 (2013) 892–902, <https://doi.org/10.1366/12-06723>.
- [40] O.E. Adedipe, T.A. Jacot, A.R. Thurman, G.F. Doncel, M.R. Clark, Rapid measures of user's adherence to vaginal drug products using attenuated total reflectance fourier transform infrared spectroscopy (ATR-FTIR) and multivariate discriminant techniques, *PLoS One* 1 (2018), e0197906, <https://doi.org/10.1371/journal.pone.0197906>.
- [41] Rstudio Team, R: A Language and Environment For Statistical Computing, R Core Team, R Foundation for Statistical Computing, Vienna, Austria, 2021.
- [42] A. Gajardo, C. Carroll, Y. Chen, X. Dai, J. Fan, P.Z. Hadjipantelis, K. Han, H. Ji, H. Mueller, J. Wang, fdpac: functional data analysis and empirical dynamics, (R package version 0.5.7), 2021.
- [43] D. Ruppert, M.P. Wand, R.J. Carroll, *Semiparametric Regression*, Cambridge University Press, Cambridge, 2003.
- [44] J. Fox, S. Weisberg, *An R Companion to Applied Regression*, 3rd ed., Sage, Thousand Oaks, 2019.
- [45] C. von Hoermann, J. Ruther, S. Reibe, B. Madea, M. Ayasse, The importance of carcass volatiles as attractants for the hide beetle *Dermestes maculatus* (De Geer), *Forensic Sci. Int.* 212 (2011) 173–179, <https://doi.org/10.1016/j.forsciint.2011.06.009>.
- [46] B.H. Stuart, S. Forbes, B.B. Dent, G. Hodgson, Studies of adipocere using diffuse reflectance infrared spectroscopy, *Vib. Spectrosc.* 24 (2000) 233–242, [https://doi.org/10.1016/S0924-2031\(00\)00097-7](https://doi.org/10.1016/S0924-2031(00)00097-7).
- [47] B.H. Stuart, L. Craft, S.L. Forbes, B.B. Dent, Studies of adipocere using attenuated total reflectance infrared spectroscopy, *Forensic Sci. Med. Pathol.* 1 (3) (2005) 197–201, <https://doi.org/10.1385/FSMP:1:3:197>.



Sharni Collins graduated in 2018 with a BSc(Hons) in Forensic Biology and Applied Forensic Chemistry from the University of Technology Sydney. In 2019 she commenced her PhD studies investigating post-mortem lipids collected in textiles as bio-markers of time since death.



Luca Maestrini Luca Maestrini is a Postdoctoral Research Fellow at the Research School of Finance, Actuarial Studies and Statistics of The Australian National University in Canberra, Australia. His research interests range from methodological and computational statistics to statistical theory, with a particular focus on variational approximations and generalized linear mixed models. He was awarded a PhD in Statistics from University of Padua, Italy, in 2019.



Maiken Ueland Maiken Ueland is an ARC Discovery Early Career Research Fellow at the Centre for Forensic Science, University of Technology Sydney, and the Deputy Director of The Australian Facility for Taphonomic Experimental Research (AFTER). She is an emerging leader in the field of forensic taphonomy, where she uses analytical, biochemical, and spectroscopic techniques to conduct human post-mortem investigations. She received her PhD from the University of Technology Sydney in 2016.



Barbara Stuart is an Associate Professor in the Centre for Forensic Science at the University of Technology Sydney. She received BSc(Hons) and MSc degrees from the University of Sydney and completed her PhD at Imperial College, University of London. She is a recognised expert and widely published author on the application of modern analytical chemical techniques, particularly vibrational spectroscopy, to forensic, archaeological and materials conservation questions .